AJNR

# Improved Detection of Target Metabolites in Brain Tumors with Intermediate TE, High SNR, and High Bandwidth Spin-Echo Sequence at 5T

Wenbo Sun, Dan Xu, YanXing Yang, Linfei Wen, Hanjiang Yu, Yaowen Xing, Xiaopeng Song, Huan Li and Haibo Xu



*AJNR Am J Neuroradiol* 2024, 45 (4) 461-467
doi: https://doi.org/10.3174/ajnr.A8150
http://www.ajnr.org/content/45/4/461

# Improved Detection of Target Metabolites in Brain Tumors with Intermediate TE, High SNR, and High Bandwidth Spin-Echo Sequence at 5T

Wenbo Sun, Dan Xu, YanXing Yang, Linfei Wen, Hanjiang Yu, Yaowen Xing, Xiaopeng Song, Huan Li, and Haibo Xu

## ABSTRACT

**BACKGROUND AND PURPOSE:** Due to high chemical shift displacement, challenges emerge at ultra-high fields when measuring metabolites using $^{1}$H-MRS. Our goal was to investigate how well the high SNR and high bandwidth spin-echo (HISE) technique perform at 5T for detecting target metabolites in brain tumors.

**MATERIALS AND METHODS:** Twenty-six subjects suspected of having brain tumors were enrolled. HISE and point-resolved spectroscopy (PRESS) single-voxel spectroscopy scans were collected with a 5T clinical scanner with an intermediate TE (TE = 144 ms). The main metabolites, including total NAA, Cr, and total Cho, were accessed and compared between HISE and PRESS using a paired Student *t* test, with full width at half maximum and SNR as covariates. The detection rate of specific metabolites, including lactate, alanine, and lipid, and subjective spectral quality were accessed and compared between HISE and PRESS.

**RESULTS:** Twenty-three pathologically confirmed brain tumors were included. Only the full width at half maximum for total NAA was significantly lower with HISE than with PRESS ($P < .05$). HISE showed a significantly higher SNR for total NAA, Cr, and total Cho compared with PRESS ($P < .05$). Lactate was detected in 21 of the 23 cases using HISE, but in only 4 cases using PRESS. HISE detected alanine in 8 of 9 meningiomas, whereas PRESS detected alanine in just 3 meningiomas. PRESS found lipid in more cases than HISE, while HISE outperformed PRESS in terms of subjective spectral quality.

**CONCLUSIONS:** HISE outperformed the clinical standard PRESS technique in detecting target metabolites of brain tumors at 5T, particularly lactate and alanine.

**ABBREVIATIONS:** Ala = alanine; CSDE = chemical shift displacement error; FWHM = full width at half maximum; 2-HG = 2-hydroxyglutarate; HISE = high bandwidth spin-echo; Lac = lactate; Lip = lipid; PRESS = point-resolved spectroscopy; RF = radiofrequency; STEAM = stimulated echo acquisition mode; SVS = single-voxel spectroscopy; t = total

Brain tumors encompass >120 different types, with some common primary tumors being highly malignant.[1] The criterion standard for clinical diagnosis of brain tumors involves pathologic testing conducted after invasive surgical resection or needle biopsy.[2] Nevertheless, the development of noninvasive diagnostic tools is necessary.

MR imaging is a crucial noninvasive imaging tool for brain tumors.[3] $^{1}$H-MRS is an MR imaging technique that enables quantitation of different metabolite profiles in vivo.[4] The $^{1}$H-MRS spectrum shows 3 primary metabolite peaks for brain tumors, which have been linked to intact glioneuronal structures (NAA), energy homoeostasis (Cr), and tumor membrane turnover and proliferation (Cho), respectively.[5] Meanwhile, depending on the metabolite patterns of tumors, lactate (Lac), alanine (Ala), and mobile lipid (Lip) may also be observed. A metabolic shift toward glycolysis has been found in tumor cells, which is known as the Warburg effect.[6] Lac is an end product of glycolysis, while Ala is a reduced partner of pyruvate formed from glycolysis.[7] Both Lac and Ala have been associated with a range of brain tumors.[7] Lip signal is linked to necrosis and apoptosis.[7] However, the routine application of $^{1}$H-MRS in detecting the above metabolites is limited by the clinical field strength, often 1.5T, which provides low SNR and spectra resolution.[8] Typically, it is difficult to resolve Lac and Ala peaks individually at 1.5T.[8]

Higher magnetic field strengths provide an opportunity for improving $^{1}$H-MRS data quality.[9] Previous studies have demonstrated the advantages of using 3T over 1.5T in diagnosing brain

Received August 10, 2023; accepted after revision November 6.

From the Departments of Radiology (W.S., H.L., H.X.) and Nuclear Medicine (D.X.), Zhongnan Hospital of Wuhan University, Wuhan, Hubei, P.R. China; and United-Imaging Healthcare (Y.Y., L.W., H.Y., Y.X., X.S.), Shanghai, China.

Wenbo Sun and Dan Xu share first authorship.

This work was supported by the National NSFC International (regional) Cooperation and Exchange Project x 82111530204; the Key R&D Program of Hubei Province x 2020BCB030; and the Improvement Project for Theranostic Ability on Difficulty Miscellaneous Disease (tumor) of the Zhongnan Hospital of Wuhan University.

Please address correspondence to Haibo Xu, MD, PhD, Department of Radiology, Zhongnan Hospital of Wuhan University, 169 East Lake Rd, Wuhan 430071, Hubei, P. R. China; e-mail: xuhaibo1120@hotmail.com

http://dx.doi.org/10.3174/ajnr.A8150

tumors with $^1$H-MRS, in terms of higher SNR, lower spectra overlap, and shorter acquisition times.[10,11] Moreover, the application of ultra-high-field (7T) MR imaging systems further enhances SNR and provides superior spatial and spectral resolution compared with 3T.[12,13] Nearby metabolites, such as 2-hydroxyglutarate (2HG), glutamate/glutamine, and $\gamma$-aminobutyric acid, could be separated and quantified at 7T.[13] Despite these advantages, higher magnetic field strengths pose some challenges related to field inhomogeneities and a larger chemical shift displacement error (CSDE); therefore, it is necessary to optimize the acquisition scheme of $^1$H-MRS when working with higher magnetic field strengths.[14,15]

Currently, in clinical practice, the standard acquisition sequences include stimulated echo acquisition mode (STEAM) and point-resolved spectroscopy (PRESS).[14] In STEAM, 3 section-selective radiofrequency (RF) pulses, each with a 90° flip angle, generate a stimulated echo, while the PRESS technique uses a 90° excitation pulse combined with 2 refocusing pulses to produce a spin-echo.[16] PRESS is preferred over STEAM due to its ability to double the signal output.[14] However, both STEAM and PRESS are susceptible to the increased CSDE at higher field strengths.[14] With increased CSDE, PRESS and STEAM would both have anomalous J-modulation, and additional signal cancellation would occur in metabolites with weakly coupled resonances, like Lac.[14] The high SNR and high bandwidth spin-echo (HISE) technique, also called semi-adiabatic localization by adiabatic selective refocusing (sLASER) by some MR imaging manufacturers, has been recently applied to overcome this challenge.[17] In HISE, the 2 refocusing pulses are replaced by 2 pairs of adiabatic full-passage pulses, allowing a higher RF pulse bandwidth, less sensitivity to field inhomogeneities, and superior section-selection profiles, decreasing the CSDE to a minimum.[17] Therefore, HISE is recommended for high and ultra-high-field applications.[14] Several investigations at 7T have already applied similar HISE approaches and proved the benefits of HISE in detecting unique compounds and resolving adjacent metabolites.[13,17-20] Nevertheless, clinical use of 7T MR imaging systems is not yet common, even though the FDA has approved the technology.[21] As a result, the clinical potential of the combination of ultra-highfield and the HISE technique has not been fully explored.

Recently, a 5T clinical scanner has also shown its capabilities in neuroimaging. In displaying the intracranial distal small branches with TOF MRA, it surpasses 3T and is comparable with 7T.[22] Additionally, 5T enables better visualization of intracranial vessels than 3T for vessel wall imaging and SWI.[23] For quantitative T1$\rho$ mapping of brain tissues, 5T showed more benefits in the SNR than 3T at a high spatial resolution.[24] It has also been demonstrated that 5T had a lower RF inhomogeneity and specific absorption rate than 7T[23] and was capable of scanning abdominal organs, including the pancreas,[25,26] kidney,[27] spleen,[28] and liver,[28] whereas 7T has not been approved for such applications, due to the RF inhomogeneity in large-body cross-sections and safety considerations concerning RF power deposition.[29] Imaging at 5T may offer a good balance between the benefits and drawbacks of ultra-high-field MR imaging and thus may see wider applicable clinical scenarios than 7T in the future.

So far, the performance of $^1$H-MRS in diagnosing brain tumors has never been investigated at 5T. Because 5T belongs to the ultra-high field, we hypothesize that HISE will show obvious advantages at 5T. The objective of this study was to validate the application of the HISE technique at 5T in the clinic and compare its performance in detecting target metabolites of brain tumors with that of the clinical standard PRESS technique.

**Table 1: Acquisition parameters for the HISE and PRESS SVS sequences**

| Parameters | HISE | PRESS |
|---|---|---|
| TR | 2500 ms | 2500 ms |
| TE | 144 ms | 144 ms |
| Voxel size | 15 ×15 ×15 mm$^3$ | 15 ×15 ×15 mm$^3$ |
| Bandwidth | 1000 kHz | 1000 kHz |
| Averages | 100 | 100 |
| Spectral sampling | 1024 | 1024 |
| Flip angle | 90° | 90° |
| Phase-cycling schemes | 2 blocks | 4 blocks |
| Water-suppressed bandwidth | 90 kHz | 90 kHz |
| Acquisition time | 4 min 19 sec | 4 min 14 sec |

**Note:**—min indicates minute; sec, second.

## MATERIALS AND METHODS

### Subjects

This prospective study was approved by the ethics committee of our hospital (ethics number 2021110). From March 2023 to July 2023, a total of 26 patients suspected of having brain tumors were enrolled in this study. Informed consent was obtained from all participants. The inclusion criteria were as follows: between 18 and 80 years of age, suspected of having brain tumors, no contraindications to MR imaging (including metal implants and claustrophobia), and no history of brain surgery, radiation therapy, or chemotherapy. The exclusion criteria comprised patients who did not undergo brain surgery after MR imaging ($n = 1$), patients who were pathologically confirmed not to have a brain tumor ($n = 1$), and incomplete image acquisition ($n = 1$).

### Image Acquisition and Analysis

All MR images were obtained using a 5T whole-body MR scanner (uMR Jupiter; United Imaging Healthcare) with a 2-channel transmit and 48-channel receive (2Tx/48Rx; United Imaging Healthcare) head coil. For both HISE and PRESS, the CSDE data were first acquired in a phantom containing 100% water. For phantom and in vivo measurements, HISE and PRESS were scanned on the basis of the parameters specified in Table 1. Before the single-voxel spectroscopy (SVS) scans, T2-weighted FSE sequences were acquired in 3 anatomic directions (sagittal, coronal, and axial) to cover the entire brain and aid in the localization of tumor lesions. The acquisition parameters for the T2-weighted FSE sequences were as follows: FOV = 230 × 200 mm$^2$, TR = 4000 ms, TE = 94 ms, section thickness = 5 mm, section number = 19, acceleration = 2.0, gap = 30%, flip angle = 90°, and resolution in-plane = 0.65 × 0.65 mm$^2$. Subsequently, HISE and PRESS SVS scans were obtained in a random order with an intermediate TE of 144 ms. An intermediate TE was used for the detection of Lac signals at 7T.[17] Before scanning, a $B_0$ shimming was performed. During scans, a dynamic frequency calibration module to correct the frequency shift during measurement and a motion-monitoring module were added.

Prominent metabolites, including total NAA (tNAA, composed of NAA and N-Acetyl-Aspartyl-Glutamate (NAAG)), Cr, and total Cho (tCho, composed of glycerophosphocholine and phosphorylcholine) were measured at chemical shift positions of 2.03, 3.03, and 3.21 ppm, respectively. The full width at half maximum (FWHM) and SNR of tNAA, Cr, and tCho were calculated using custom-designed software. The FWHM was used to evaluate the quality of shimming and was measured from the spectral width at the half amplitude of the metabolite signal. The SNR was calculated using the highest baseline subtracted metabolite signal intensity divided by the SD of the noise on the spectral baseline estimated from a region free from metabolite signals. To detect specific metabolites, we used an in-house MATLAB script (MathWorks) for spectra editing. Lac, Ala, and Lip signals were detected at 1.34, 1.45, and 1.3 ppm, respectively. A comparative analysis of the detection rate in Lac, Ala, and Lip signals between HISE and PRESS was performed. Moreover, the overall spectral quality of HISE and PRESS for each subject was rated by 2 radiologists with 5 and 10 years of experience, using a 5-point Likert scale. The Likert scale was used with the following grades: 1 = not diagnostic; 2 = spectra are markedly distorted with poor diagnostic value; 3 = spectra are minimally distorted with reduced diagnostic value; 4 = no distortion with good diagnostic value; and 5 = spectra with excellent diagnostic quality by presenting more peaks of metabolites. The 2 radiologists reached a consensus over the scores.

### Pathologic Analysis

After surgery, tumor specimens were fixed in 4% paraformaldehyde, embedded in paraffin, and sectioned into 4 -$\mu$m-thick histologic sections for pathologic diagnosis. Both routine H&E staining and immunohistochemistry analysis were performed. Additionally, DNA sequencing was performed to confirm the presence of gene mutations for gliomas, including the *IDH* mutation and 1p/19q codeletion. The diagnosis was made by a pathologist with 10 years of experience following the guidelines outlined in the 2016 World Health Organization Classification of Tumors of the Central Nervous System.

### Statistical Analysis

To compare the FWHM and SNR of tNAA, Cr, and tCho between 2 scans, we used a paired Student *t* test. The detection rate of Lac, Ala, and Lip signals among all cases was calculated for both sequences. For the evaluation of spectral quality, the Likert scale was compared between HISE and PRESS with frequency tables and a paired Student *t* test. All statistical analyses were performed using SPSS Version 24.0 software (IBM). A $P$ value $< .05$ suggested a statistically significant difference.

## RESULTS

A total of 23 patients (mean age, 55.39 [SD, 11.17] years, male, $n = 8$) were finally included in this study, with tumors consisting of acoustic neuroma ($n = 2$), non-Hodgkin lymphoma ($n = 1$), meningiomas ($n = 9$), gliomas ($n = 9$), and metastasis ($n = 2$).

### CSDE for HISE and PRESS with 5T

Due to the high bandwidth property of the adiabatic pulse, the phantom experiment showed a obviously reduced CSDE with 5T (3.5%/ppm for the adiabatic refocusing pulse) compared with a normal PRESS sequence (15.3%/ppm), as shown in Fig 1.

### FWHM and SNR of Prominent Target Metabolites

As shown in Table 2, the FWHM for tNAA was significantly lower with HISE than with PRESS ($P < .05$), while the SNR for tNAA, Cr, and tCho was significantly higher with HISE compared with PRESS ($P < .05$).

### Detection Rate of Specific Target Metabolites

As shown in Table 3, among all brain tumors, HISE detected Lac in 21 cases, whereas PRESS detected Lac in just in 4 cases. HISE detected Ala in 8 of 9 meningiomas, while PRESS detected Ala in only 3 meningiomas. PRESS detected Lip signals in 14 cases, while HISE detected Lip signals in 11 cases.

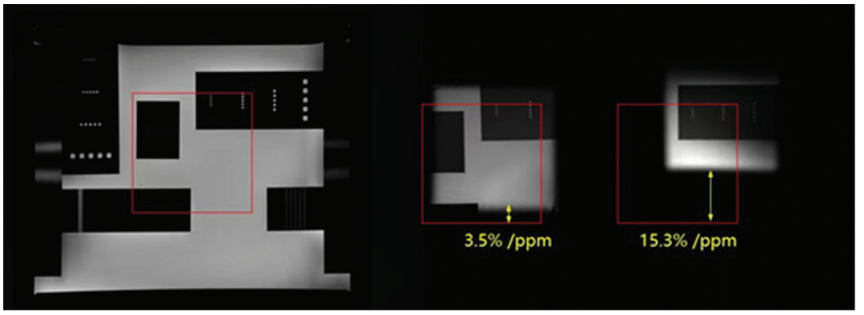


**FIG 1.** A comparison of CSDE with HISE and PRESS in a phantom containing 100% water. The *red square* indicates the FOV in the center of the phantom, while the *middle image* is the result of HISE, and the *right image* is the result of PRESS.

**Table 2: A comparison of average values (mean [SD]) of FWHM and SNR of prominent metabolites for the HISE and PRESS SVS scans among all cases[a]**

| | FWHM | | | SNR | | |
|---|---|---|---|---|---|---|
| Metabolite | HISE | PRESS | *P* Value | HISE | PRESS | *P* Value |
| tNAA | 10.92 (SD, 2.59) | 14.12 (SD, 3.62) | .001[b] | 14.61 (SD, 7.66) | 9.53 (SD, 5.48) | .001[b] |
| Cr | 10.87 (SD, 3.31) | 11.75 (SD, 4.72) | .455 | 20.02 (SD, 14.06) | 9.44 (SD, 6.12) | .000[c] |
| tCho | 12.07 (SD, 2.74) | 12.74 (SD, 3.45) | .215 | 63.23 (SD, 43.32) | 29.72 (SD, 19.19) | .000[c] |

[a] The *P* value shown is for the paired *t* test performed between HISE and PRESS.
[b] $P < .01$.
[c] $P < .001$.

**Table 3: The detection of specific metabolites (Lac, Ala, and Lip) at TE = 144 ms for the HISE and PRESS SVS scans, respectively[a]**

| No. | Sex | Age (yr) | Pathologic Diagnosis | HISE | | | PRESS | | |
|---|---|---|---|---|---|---|---|---|---|
| | | | | Lac | Ala | Lip | Lac | Ala | Lip |
| Case 1 | F | 71 | Acoustic neuroma | + | – | + | – | – | + |
| Case 2 | M | 47 | Acoustic neuroma | + | – | – | – | – | – |
| Case 3 | M | 52 | Metastases (lung origin) | + | ? | + | – | – | + |
| Case 4 | M | 58 | Metastases (gastrointestinal origin) | + | – | + | – | – | + |
| Case 5 | M | 61 | Non-Hodgkin lymphoma | + | – | + | – | – | + |
| Case 6 | M | 66 | Meningioma, WHO I | + | + | – | – | – | – |
| Case 7 | F | 52 | Meningioma, WHO I | + | + | – | – | – | – |
| Case 8 | F | 67 | Meningioma, WHO I | + | ? | – | + | – | – |
| Case 9 | F | 43 | Meningioma, WHO II | + | + | – | – | + | – |
| Case 10 | M | 52 | Meningioma, WHO I | + | ? | + | – | – | + |
| Case 11 | F | 34 | Meningioma, WHO I | + | + | – | – | ? | – |
| Case 12 | F | 56 | Meningioma, WHO I | – | – | + | – | – | + |
| Case 13 | F | 50 | Meningioma, WHO I | + | + | – | – | – | – |
| Case 14 | F | 58 | Meningioma, WHO I | – | + | + | – | ? | + |
| Case 15 | F | 42 | Oligodendroglioma, WHO III | + | – | – | – | – | – |
| Case 16 | F | 49 | Oligodendroglioma, WHO II | + | – | – | – | – | – |
| Case 17 | F | 35 | GBM, WHO IV | + | – | – | – | – | + |
| Case 18 | M | 45 | GBM, WHO IV | + | ? | + | – | – | + |
| Case 19 | F | 64 | GBM, WHO IV | + | ? | + | + | – | + |
| Case 20 | F | 67 | GBM, WHO IV | + | – | – | – | – | + |
| Case 21 | F | 70 | GBM, WHO IV | + | ? | + | – | – | + |
| Case 22 | M | 66 | GBM, WHO IV | + | – | – | + | – | + |
| Case 23 | F | 69 | GBM, WHO IV | + | – | + | + | – | + |

**Note:**—F indicates female; M, male; WHO, World Health Organization; GBM, glioblastoma.
[a] The plus sign represents the detection of strong signal peaks; the question mark represents the presence of faint or inconspicuous signal peaks; and the minus sign represents the almost undetectable signal peaks.

**Table 4: A comparison of results of spectral quality rating between HISE and PRESS SVS**

| Rate | HISE SVS | PRESS-SVS | *P* Value |
|---|---|---|---|
| 1 | 0 | 0 | NA |
| 2 | 0 | 2 | NA |
| 3 | 2 | 8 | NA |
| 4 | 5 | 8 | NA |
| 5 | 16 | 5 | NA |
| Mean value | 4.61 (SD, 0.66) | 3.70 (SD, 0.93) | .001[a] |

**Note:**—NA indicates not applicable.
[a] $P < .01$.

### *Subjective Spectral Quality Evaluations*

The HISE showed significantly higher scores in spectral quality than PRESS ($P < .001$), as demonstrated in Table 4. Representative spectra for typical patients (meningioma, glioma, metastases, and acoustic neuroma) are demonstrated in Figs 2–5, respectively.

## DISCUSSION

This study aimed to investigate the performance of HISE in diagnosing brain tumors with a 5T ultra-high-field whole-body clinical scanner by comparing HISE with the clinical standard PRESS. We found that HISE demonstrated significantly higher SNR in tNAA, Cr and tCho compared with PRESS. Furthermore, we observed a higher detection rate of Lac signal in all tumors, as well as a higher detection rate of Ala in meningiomas with HISE. In addition, PRESS showed a higher detection rate for Lip signals. According to the 5-point Likert scale, a significant, higher spectral quality with HISE than with PRESS was found. Altogether, these findings suggested that the application of HISE holds promise in clinical settings for diagnosing brain tumors with a recently developed 5T clinical scanner.

Several studies have already compared HISE or similar techniques with PRESS at 3T.[30,31] A prior study compared HISE with PRESS and discovered that HISE has a lower CSDE than PRESS (6% versus 24%) and a stronger signal of mIns and Cr in its spectra than PRESS.[30] Another study compared similar techniques, Mescher-Garwood (MEGA) semi-localised by adiabatic selective refocusing (MEGA-sLASER) and MEGA-PRESS at Siemens 3T system, and found obvious SNR increases (mean, 10.9 [SD, 5.2] versus 5.0 [SD, 3.0]) using MEGA-sLASER for Lac detection in distinct brain areas.[31] Meanwhile, only a few studies have looked into PRESS at 7T, which could be due to the drawback of PRESS at high fields, a very high CSDE due to a constricted refocusing pulse bandwidth.[32] An earlier investigation in 12 patients with gliomas found that a modified PRESS sequence could detect 2HG and separate it from glutamate/glutamine and $\gamma$-aminobutyric acid signals.[33] However, it showed a large CSDE (20%) of PRESS at 7T.[33]

In comparison with the scant literature on PRESS at 7T, many studies have focused on the use of HISE in neuroimaging at 7T.[13,18-20,34] A study on 5 healthy volunteers with HISE found an average SNR (48 [SD, 6]) for NAA and reliable readings for Cho, NAA, Cr, mIns, and glutamate/glutamine.[18] Another study used HISE in 7 gliomas and found an average SNR (24.4 [SD, 13.6]) for the obtained spectra in tumor locations, and 8 metabolites, including lactate, NAA, Cho, and Cr, could be identified.[20] HISE was also shown to be capable of detecting 2HG with an average SNR (77 [SD, 26]) in a study involving 9 patients with gliomas[13] and detected 2HG concentration as low as 0.5 mM in a study involving 4 *IDH1* mutant glioms.[34] In addition, a study on healthy volunteers using an HISE sequence at 7T revealed high

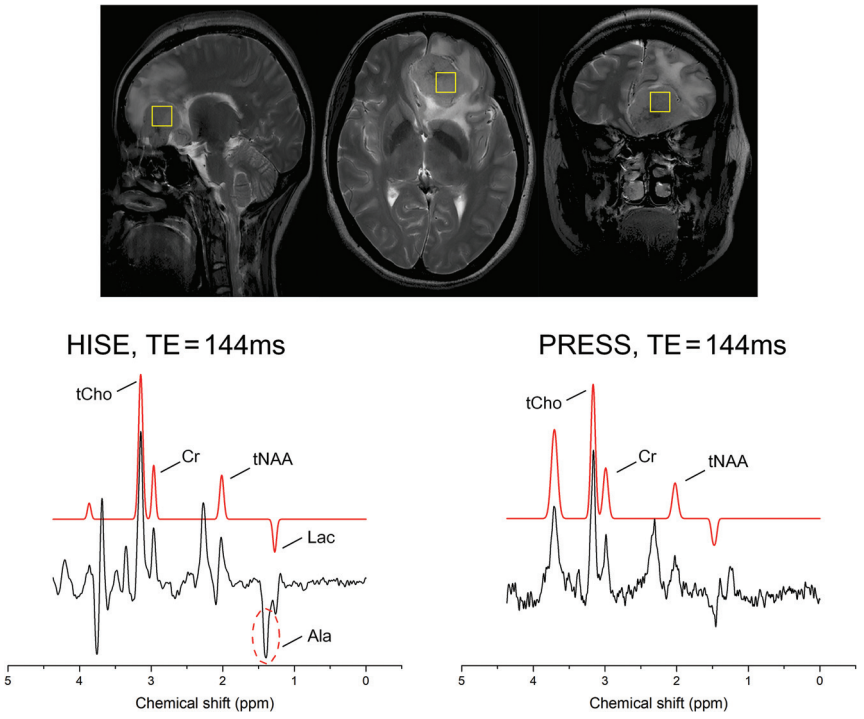


**FIG 2.** A 43-year-old woman with a mass located in the left frontal lobe, suggesting a meningioma. It was an atypical meningioma (World Health Organization grade II) with invasion into the brain parenchyma. The HISE technique observed relatively strong Ala signal, while the PRESS technique could not differentiate between the Ala and Lac peaks. Both HISE and PRESS did not detect Lip signals. The *yellow box* in anatomical images represented the region of the volume of the SVS scan.

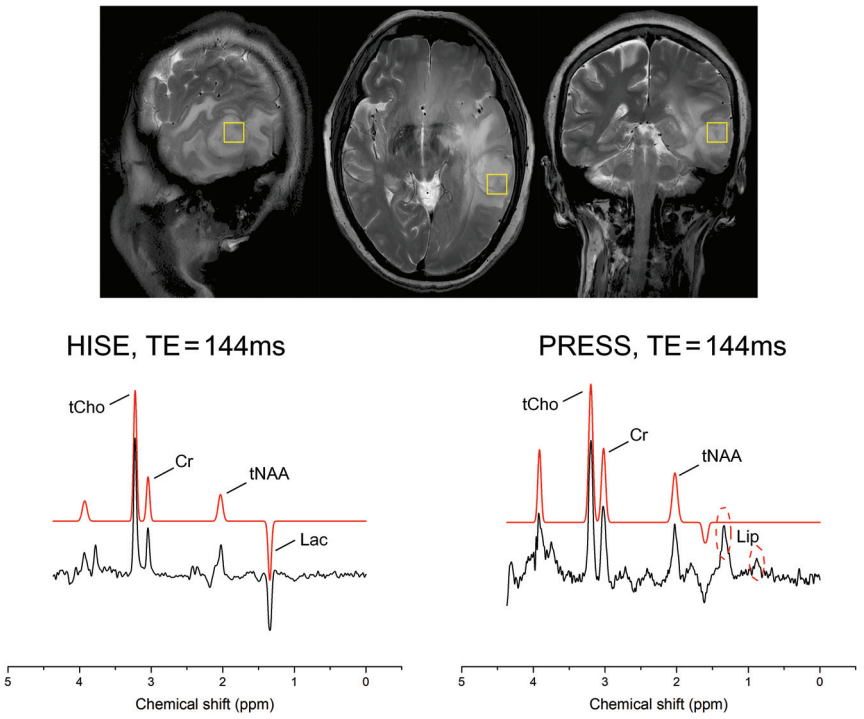


**FIG 3.** A 67 -year-old woman with a mass in the left temporal lobe with surrounding edema. On the basis of multimodal MR imaging, a high-grade glioma was suspected. Clinical correlation was recommended. The glioma was classified as a glioblastoma (World Health Organization grade IV, *IDH1* wild-type). In the HISE, a Lac signal was detected. In PRESS, due to chemical shift displacement effects, a Lip signal originating from the scalp was detected, and the Lac signal was covered by the Lip signal. The *yellow box* in anatomical images represented the region of the volume of the SVS scan.

SNR (mean, 119 [SD, 39]) and well-fitting results for brain glutamate.[19] These findings at 7T support the experts' consensus that ultra-high fields generally favor HISE over PRESS; however, these results have never been repeated at 5T, and there is little evidence for the routine use of HISE for brain tumors at 5T. Hence, a comparison study of HISE and PRESS at 5T is still essential.

At ultra-high field, inhomogeneities ($B_0$ and $B_1$) are prevalent and may have an influence on the quality of the $^1$H-MRS spectrum. FWHM is an important indicator of the $B_0$ shimming.[35] In our study, we found a similar or better $B_0$ shimming with HISE than PRESS at 5T, despite the lesions being located near the base of the skull or scalp, which could be influenced by susceptibility artifacts. Moreover, we found significantly higher SNR in tNAA, Cr, and tCho when using HISE compared with PRESS at 5T. These results indicate that at 5T, HISE may still show advantages over PRESS in terms of SNR. It might be due to the following reasons:[32] When the magnetic field strength increases, a larger RF field is needed to flip the spin. Due to the limitation of the RF field amplitude of the system and to minimize CSDE, the return flip angle of the PRESS sequence is usually $<180°$. However, by using an adiabatic refocusing pulse in the HISE sequence, the return flip angle can reach 180° under the same condition, resulting in a lower sensitivity to field inhomogeneities and a higher SNR.

Besides SNR, we observed a higher detection rate of Lac and Ala using HISE compared with PRESS at 5T. Lac accumulation serves as an important marker of bulk tumors.[36] According to the hypothesis of the Warburg effect, increased Lac levels may be caused by increased glycolysis and hypoxia in tumors.[6] However, the limited detection rate of Lac in PRESS can be because Lac is a metabolite with frequency-separated J-coupled multiplets.[14] As a result, it may experience signal loss in PRESS due to the unequal exposure of regions around the voxel edge periphery to two 180° refocusing pulses.[14] HISE increased the bandwidth of the RF pulses, thus reducing the signal cancellation in Lac.[17]

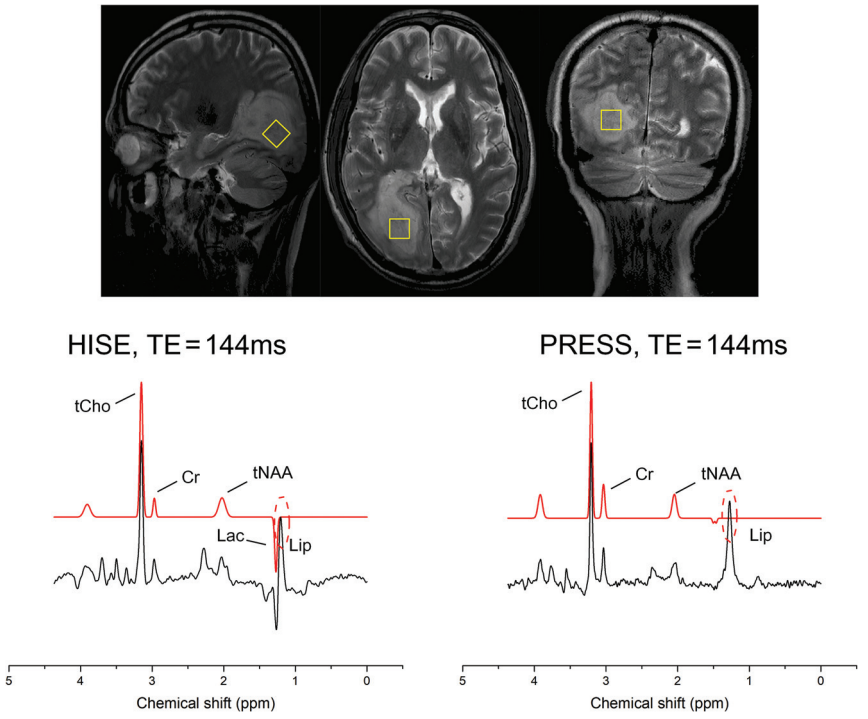


**FIG 4.** A 52-year-old man with a right occipital lobe space-occupying lesion, which was classified as a brain metastasis (originating from lung cancer). In the HISE, both Lac and Lip signals were detected. In PRESS, only a Lip signal was detected, and the Lac signal was covered by the Lip signal. The *yellow box* in anatomical images represented the region of the volume of the SVS scan.

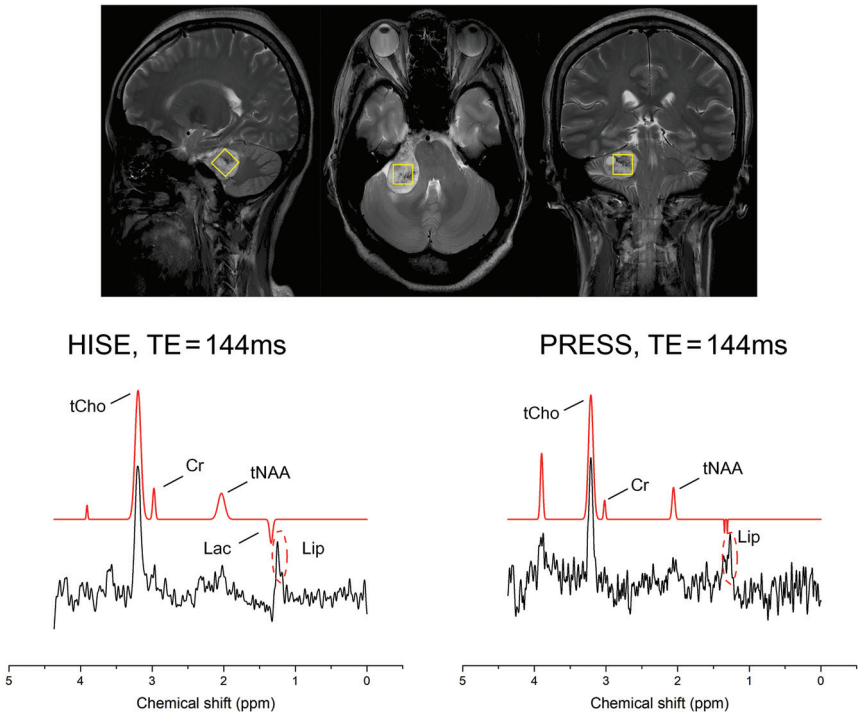


**FIG 5.** A 71-year-old woman with a space-occupying lesion in the right cerebellopontine angle, confirmed to be an acoustic neuroma after surgery. In the HISE, a small Lac signal was detected, In PRESS, the Lac signal was also covered by the Lip signal. The *yellow box* in anatomical images represented the region of the volume of the SVS scan.

Additionally, we detected more Ala cases with HISE in gliomas and meningiomas. Ala could enter the metabolic stream to provide energy and precursors for rapidly proliferating tumor cells in gliomas.[37] Furthermore, because Ala is a hallmark of meningioma,[8] the high detection rate of Ala in meningiomas could be attributed to the enhanced spectral resolution and less CSDE of HISE at 5T, as shown in Fig 2. Last, PRESS showed more cases with Lip signals. This could be owing to the difficulty of PRESS in completely suppressing scalp Lip signals, as demonstrated in Fig 3. However, compared with PRESS, HISE has superior section-selection characteristics, thus reducing Lip contaminations from outside the measurement volume.[30]

Some limitations of this study should be acknowledged. First, the size of our research cohort was relatively small. A larger sample size would provide more statistical power and enhance the generalizability of the findings. Second, we did not conduct reliable and reproducible comparisons of these 2 sequences between 3T and 5T. Although it is common sense that a higher field strength would have a higher CSDE, further investigations comparing the 2 sequences between 3T and 5T are warranted. Third, we chose only an intermediate TE (144 ms), which is recommended at 7T for the detection of negative in-phase Lac.[17] A shorter TE could be achieved by PRESS than by HISE, which could reduce the signal loss due to T2 relaxation. A further comparison study using shorter TEs toward other metabolites, 2HG, which is crucial for the diagnosis of isocitrate dehydrogenase mutant gliomas, is planned at 5T. Last, we evaluated only the SVS scans. Although SVS has been proved to be robust in clinical settings, particularly for most lesions located at anatomic regions with $B_0$ field inhomogeneities in our cohort, it would be beneficial to investigate the HISE technique based on a 2D or 3D chemical shift imaging approach. This process would provide a more comprehensive understanding of the performance of the HISE technique at 5T.

## CONCLUSIONS

In a recently developed whole-body 5T clinical scanner, the HISE technique is preferable to PRESS for the clinical diagnosis of brain tumors. This result is attributed to its higher SNR and detection rate of target metabolites in brain tumors, especially Lac and Ala.


## ACKNOWLEDGMENTS

We would like to express our gratitude to Prof. Qu Xiaobo and Dr. Tu Zhangren from Xiamen Univerisy for their assistance in testing the data for 2HG detection using the LCModel.

Disclosure forms provided by the authors are available with the full text and PDF of this article at www.ajnr.org.


## REFERENCES


1. Mack SC, Hubert CG, Miller TE, et al. **An epigenetic gateway to brain tumor cell identity.** *Nat Neurosci* 2016;19:10–19 CrossRef Medline
2. Di Bonaventura R, Montano N, Giordano M, et al. **Reassessing the role of brain tumor biopsy in the era of advanced surgical, molecular, and imaging techniques-a single-center experience with long-term follow-up.** *J Pers Med* 2021;11:909 CrossRef Medline
3. Haubold J, Demircioglu A, Gratz M, et al. **Non-invasive tumor decoding and phenotyping of cerebral gliomas utilizing multiparametric 18F-FET PET-MRI and MR fingerprinting.** *Eur J Nucl Med Mol Imaging* 2020;47:1435–45 CrossRef Medline
4. Bednarik P, Goranovic D, Svatkova A, et al. **$^{1}$H magnetic resonance spectroscopic imaging of deuterated glucose and of neurotransmitter metabolism at 7 T in the human brain**. *Nat Biomed Eng* 2023;7:1001–13 CrossRef Medline
5. Wang Q, Zhang H, Zhang J, et al. **The diagnostic performance of magnetic resonance spectroscopy in differentiating high-from low-grade gliomas: a systematic review and meta-analysis.** *Eur Radiol* 2016;26:2670–84 CrossRef Medline
6. Gatenby RA, Gillies RJ. **Why do cancers have high aerobic glycolysis?** *Nat Rev Cancer* 2004;4:891–99 CrossRef Medline
7. Griffin JL, Kauppinen RA. **A metabolomics perspective of human brain tumours.** *FEBS J* 2007;274:1132–39 CrossRef Medline
8. Krishnamoorthy T, Radhakrishnan VV, Thomas B, et al. **Alanine peak in central neurocytomas on proton MR spectroscopy.** *Neuroradiology* 2007;49:551–54 CrossRef Medline
9. Maudsley AA, Andronesi OC, Barker PB, et al. **Advanced magnetic resonance spectroscopic neuroimaging: experts' consensus recommendations**. *NMR Biomed* 2021;34:e4309 CrossRef Medline
10. Kim JH, Chang KH, Na DG, et al. **Comparison of 1.5T and 3T 1H MR spectroscopy for human brain tumors.** *Korean J Radiol* 2006;7:156–61 CrossRef Medline
11. Sjøbakk TE, Lundgren S, Kristoffersen A, et al. **Clinical $^{1}$H magnetic resonance spectroscopy of brain metastases at 1.5T and 3T**. *Acta Radiol* 2006;47:501–08 CrossRef Medline
12. McCarthy L, Verma G, Hangel G, et al. **Application of 7T MRS to high-grade gliomas.** *AJNR Am J Neuroradiol* 2022;43:1378–95 CrossRef Medline
13. Berrington A, Voets NL, Larkin SJ, et al. **A comparison of 2-hydroxyglutarate detection at 3 and 7 T with long-TE semi-LASER.** *NMR Biomed* 2018;31 CrossRef Medline
14. Wilson M, Andronesi O, Barker PB, et al. **Methodological consensus on clinical proton MRS of the brain: review and recommendations.** *Magn Reson Med* 2019;82:527–50 CrossRef Medline
15. Henning A. **Proton and multinuclear magnetic resonance spectroscopy in the human brain at ultra-high field strength: a review.** *Neuroimage* 2018;168:181–98 CrossRef Medline
16. Bingölbali A, Fallone BG, Yahya A. **Comparison of optimized long echo time STEAM and PRESS proton MR spectroscopy of lipid olefinic protons at 3 Tesla**. *J Magn Reson Imaging* 2015;41:481–86 CrossRef Medline
17. Fernandes CC, Lanz B, Chen C, et al. **Measurement of brain lactate during visual stimulation using a long TE semi-LASER sequence at 7 T.** *NMR Biomed* 2020;33:e4223 CrossRef Medline
18. Penner J, Bartha R. **Semi-LASER $^{1}$H MR spectroscopy at 7 Tesla in human brain: metabolite quantification incorporating subject-specific macromolecule removal.** *Magn Reson Med* 2015;74:4–12 CrossRef Medline
19. Wong D, Schranz AL, Bartha R. **Optimized in vivo brain glutamate measurement using long-echo-time semi-LASER at 7 T.** *NMR Biomed* 2018;31:e4002 CrossRef Medline
20. Prener M, Opheim G, Shams Z, et al. **Single-voxel MR spectroscopy of gliomas with s-LASER at 7T.** *Diagnostics (Basel)* 2023;13:1805 CrossRef
21. Jones SE, Lee J, Law M. **Neuroimaging at 3T vs 7T: is it really worth it?** *Magn Reson Imaging Clin N Am* 2021;29:1–12 CrossRef Medline
22. Shi Z, Zhao X, Zhu S, et al. **Time-of-flight intracranial MRA at 3 T versus 5 T versus 7 T: visualization of distal small cerebral arteries.** *Radiology* 2022;305:E72 CrossRef Medline
23. Wei Z, Chen Q, Han S, et al. **5T magnetic resonance imaging: radio frequency hardware and initial brain imaging.** *Quant Imaging Med Surg* 2023;13:3222–40 CrossRef Medline
24. Liu Y, Wang W, Zheng Y, et al. **Magnetic resonance T1$\rho$ quantification of human brain at 5.0 T: a pilot study**. *Front Phys* 2022;10:1016932 CrossRef
25. Jiang Z, Sun W, Xu D, et al. **Stability and repeatability of diffusion-weighted imaging (DWI) of normal pancreas on 5.0 Tesla magnetic resonance imaging (MRI).** *Sci Rep* 2023;13:11954 CrossRef Medline
26. Zheng L, Yang C, Liang L, et al. **T2-weighted MRI and reduced-FOV diffusion-weighted imaging of the human pancreas at 5 T: a comparison study with 3 T.** *Med Phys* 2023;50:344–53 CrossRef Medline
27. Zheng L, Yang C, Sheng R, et a. **Renal imaging at 5 T versus 3 T: a comparison study.** *Insights Imaging* 2022;13:155 CrossRef Medline
28. Zhang Y, Yang C, Liang L, et al. **Preliminary experience of 5.0 T higher field abdominal diffusion-weighted MRI: agreement of apparent diffusion coefficient with 3.0 T imaging**. *J Magn Reson Imaging* 2022;56:1009–17 CrossRef Medline
29. Kraff O, Quick HH. **7T: physics, safety, and potential clinical applications.** *J Magn Reson Imaging* 2017;46:1573–89 CrossRef Medline
30. Scheenen TW, Klomp DW, Wijnen JP, et al. **Short echo time 1H-MRSI of the human brain at 3T with minimal chemical shift displacement errors using adiabatic refocusing pulses.** *Magn Reson Med* 2008;59:1–6 CrossRef Medline
31. Dacko M, Lange T. **Improved detection of lactate and $\beta$-hydroxybutyrate using MEGA-sLASER at 3 T**. *NMR Biomed* 2019;32:e4100 CrossRef Medline
32. Fuchs A, Luttje M, Boesiger P, et al. **SPECIAL semi-LASER with lipid artifact compensation for 1H MRS at 7 T.** *Magn Reson Med* 2013;69:603–12 CrossRef Medline
33. Ganji SK, An Z, Tiwari V, et al. **In vivo detection of 2-hydroxyglutarate in brain tumors by optimized point-resolved spectroscopy (PRESS) at 7T.** *Magn Reson Med* 2017;77:936–44 CrossRef Medline
34. Shams Z, van der Kemp WJ, Emir U, et al. **Comparison of 2-hydroxyglutarate detection with sLASER and MEGA-sLASER at 7T.** *Front Neurol* 2021;12:718423 CrossRef Medline
35. Enoki T, Jomoto W, Yamano T, et al. **Influences of tumor volume and FWHM of the water peak and T2* value of water on the detection rate of the choline peaks in proton MR spectroscopy of breast cancer at 3.0 T-MRI [in Japanese]**. *Nihon Hoshasen Gijutsu Gakkai Zasshi* 2021;77:351–57 CrossRef Medline
36. Li X, Yang Y, Zhang B, et al. **Lactate metabolism in human health and disease.** *Signal Transduct Target Ther* 2022;7:305 CrossRef Medline
37. Ijare O, Baskin D, Pichumani K. **CBMT-01: alanine fuels energy metabolism of glioblastoma cells.** *Neuro Oncol* 2019;21:vi32–33 CrossRef